# Synthesis, Magnetism, and Electrical Properties of $La_{1-x}Ba_xTiO_3$ ($0.0 \leq x \leq 0.5$)

Joseph E. Sunstrom, IV and Susan M. Kauzlarich*

*Department of Chemistry, University of California, Davis, California 95616*

*Received February 24, 1993. Revised Manuscript Received July 30, 1993®*

The study of cation substitution in transition-metal oxides provides fundamental information needed to understand such phenomena as high-$T_c$ superconductivity and magnetic order in oxide materials. The solid solution $La_{1-x}Ba_xTiO_3$ ($0.0 \leq x \leq 0.5$) has been prepared by arc melting stoichiometric amounts of $LaTiO_3$ and $BaTiO_3$ under argon. Single-phase samples can be made for the stoichiometry range studied here. The polycrystalline samples have been characterized using electron microprobe, thermal gravimetric analysis, temperature- and field-dependent magnetization, and dc resistivity. The stoichiometries determined by microprobe agree well with the theoretical stoichiometries. $LaTiO_3$ is a canted antiferromagnet which shows a net ferromagnetic ordering at 150 K. The ferromagnetic order is destroyed with the addition of 5% $BaTiO_3$. All of the $La_{1-x}Ba_xTiO_3$ ($x > 0$) samples exhibit temperature-independent magnetism in the high-temperature (160–300 K) range and paramagnetism in the low temperature (<50 K) region. The $La_{1-x}Ba_xTiO_3$ samples display poor metallic conductivity. In addition, several random samples display a sharp drop in resistivity which is reminiscent of PTCR thermistor behavior.

## Introduction

A large body of research has been completed on superconducting copper and bismuth oxides, but it is still not well understood why these compounds superconduct. In a more basic approach, Torrance et al. have sought to understand why some metal oxides are conductors and others are insulators.[1,2] We have initiated a study of titanium oxides that become metallic through cation substitution, but do not exhibit superconductivity or magnetic order. Specifically, our interest has been the substitution of alkaline earth cations into metallic rare earth titanates $RTiO_3$ (R = La, Ce) to understand the effect of the alkaline earth/rare earth metal cations on the magnetic and electrical properties.[3-6] Our previous results have shown that materials with the same average titanium valence, for example, $Ce_{0.8}Sr_{0.2}TiO_3$ and $Ce_{0.8}Ba_{0.2}TiO_3$,[3] can have remarkably different properties. This leads one to believe that the properties are influenced by the alkaline-earth metal cation and its inherent properties (cation radius, electronegativity, polarizability).

The doping of lanthanum into $BaTiO_3$ has also been studied extensively because polycrystalline samples exhibit a resistive anomaly at the ferroelectric Curie temperature of $BaTiO_3$.[7-10] The resistive anomaly consists of a large PTCR (positive temperature coefficient of resistance) effect. This effect can be manipulated to fabricate devices such as thermal switches. An earlier study of samarium-doped $BaTiO_3$ showed that the PTCR effect occurred only in polycrystalline samples and not in single crystals.[11] The electrical properties of the grain boundaries have been the basis for the two most accepted theoretical models.[12,13] The PTCR effect has been shown to be dependent on the method of processing and the chemical composition of the samples.[7-11,14-23] However, it is still not clear how the processing and compositional parameters (e.g., cooling rate, sintering temperature, grain size, stoichiometry) fit into the models proposed for the PTCR effect.[14]

There have been many studies on $LaTiO_3$[24-37] and

® Abstract published in *Advance ACS Abstracts*, September 15, 1993.

(1) Torrance, J. B. *J. Solid State Chem.* **1992**, *96*, 8209.
(2) Torrance, J. B.; Lacorre, P.; Asavaroengchai, C.; Metzger, R. M. *Physica C* **1991**, *182*, 351.
(3) Sunstrom, J. E., IV; Kauzlarich, S. M.; Antonio, M. R. *Chem. Mater.* **1993**, *5*, 182.
(4) Sunstrom, J. E., IV; Kauzlarich, S. M.; Klavins, P. *Chem. Mater.* **1992**, *4*, 346.
(5) Sunstrom, J. E., IV; Kauzlarich, S. M. *Mater. Res. Soc. Symp. Proc.* **1992**, *271*, 107.
(6) Kauzlarich, S. M.; Sunstrom, J. E.; Klavins, P. In *International Conference of the Chemistry of Electronic Ceramic Materials*; NIST: Jackson, WY, 1991; p 217.
(7) Gallagher, P. K.; Schey, F.; DiMarcello, F. *J. Am. Ceram. Soc.* **1963**, *46*, 359.
(8) Ryan, F. M.; Subbarao, E. C. *App. Phys. Lett.* **1962**, *1*, 69.
(9) Sauer, H. A.; Fischer, J. R. *J. Am. Ceram. Soc.* **1960**, *46*, 49.
(10) Saburi, O. *J. Phys. Soc. Jpn.* **1959**, *14*, 1159.
(11) Goodman, G. *J. Am. Ceram. Soc.* **1963**, *46*, 49.
(12) Jonker, G. H. *Solid-State Electron.* **1964**, *7*, 895.
(13) Heywang, W. *Solid-State Electron.* **1961**, *3*, 51.
(14) Ravi, V.; Kutty, T. R. N. *Mater. Sci. Eng. B* **1991**, *10*, 41.
(15) Lin, T.-F.; Hu, C.-T.; Lin, I.-N. *J. Am. Ceram. Soc.* **1990**, *73*, 531.
(16) Howng, W. Y.; McCutcheon, C. *Am. Ceram. Soc. Bull.* **1983**, *62*, 231.
(17) Kuwabara, M. J. *Am. Ceram. Soc.* **1981**, *64*, C-170.
(18) Kuwabara, M. *J. Am. Ceram. Soc.* **1981**, *64*, 639.
(19) Fukami, T.; Tsuchiya, H. *Jpn. J. Appl. Phys.* **1979**, *18*, 735.
(20) Ueoka, H.; Yodogawa, M. *IEEE Trans. Manuf. Technol.* **1974**, *MFT-3*, 77.
(21) Matsuoka, T.; Matsuo, Y.; Sasaki, H.; Hayakawa, S. *J. Am. Ceram. Soc.* **1972**, *55*, 104.
(22) Kahn, M. *Am. Ceram. Soc. Bull.* **1971**, *50*, 676.
(23) Ashida, T.; Toyoda, H. *Jpn. J. Appl. Phys.* **1966**, *5*, 269.
(24) Lichtenberg, F.; Widmer, D.; Bednorz, J. G.; Williams, T.; Reller, A. Z. Z. *Phys. B: Condens. Matter* **1991**, *82*, 211.
(25) Crandles, D. A.; Timusk, T.; Greedan, J. E. *Phys. Rev. B: Condens. Matter* **1991**, *44*, 13250.
(26) Eitel, M.; Greedan, J. E. *J. Less-Common Met.* **1986**, *116*, 95.
(27) Greedan, J. E. *J. Less-Common Met.* **1985**, *111*, 335.
(28) Goral, J. P.; Greedan, J. E. *J. Magn. Magn. Mater.* **1983**, *37*, 315.
(29) Greedan, J. E. In *The Rare Earths in Modern Science and Technology*; McCarthy, H. E., Rhyne, J. J., Eds.; Plenum: New York 1982; Vol. 3.
(30) MacLean, D. A.; Greedan, J. E. *Inorg. Chem.* **1981**, *20*, 1025.
(31) MacLean, D. A.; Ng, H.-N.; Greedan, J. E. *J. Solid State Chem.* **1979**, *30*, 35.
(32) Bazuev, G. V.; Shveikin, G. P. *Izv. Akad. Nauk SSR Neorg. Mater.* **1978**, *14*, 267.

0897-4756/93/2805-1539$04.00/0 

Table I. Lattice Parameters for $La_{1-x}Ba_xTiO_3$

| x | a (Å) | b (Å) | c (Å) | vol (Å$^3$) |
|---|---|---|---|---|
| 0.0 | 5.629(2) | 5.612(1) | 7.914(1) | 250.02(12 |
| 0.05 | 5.593(3) | 5.570(3) | 7.903(5) | 247.24(25) |
| 0.1 | 5.599(2) | 5.586(1) | 7.895(3) | 246.90(21) |
| 0.2 | 5.592(2) | 5.587(3) | 7.891(2) | 246.58(15) |
| 0.3 | 5.588(1) | 5.589(1) | 7.913(2) | 247.30(19) |
| 0.4 | 5.595(2) | 5.590(2) | 7.921(2) | 247.75(29) |
| 0.5 | 5.578(4) | 5.629(3) | 7.920(1) | 248.67(21) |

$BaTiO_3$, as well as two previous studies on $La_{1-x}Ba_xTiO_3$[38,39] prepared in a similar manner to this study. Johnston and Sestrich first completed a study on the synthesis, structure, and thermoelectric power of the $La_{1-x}Ba_xTiO_3$ system in 1961.[39] The structure of the compounds has been assigned as cubic. A recent study of the system by Eylem et al. also assigns the compounds to be cubic and biphasic.[38] Samples with the composition $0.1 \leq x \leq 0.3$ were proposed to be biphasic based on HREM studies. This group has also investigated the synthesis, structure, and properties of the $La_{1-x}Ba_xTiO_3$ system.[5] Although our magnetic property measurements appear to be in agreement with those of Eylem et al.,[38] we assign the structures to an orthorhombic system. In addition, this paper presents more details on the magnetic and electronic properties for $0.0 \leq x \leq 0.5$ and compares our results to the previous work on this system. Samples with stoichiometries greater than $x = 0.5$ are less homogeneous and prone to oxygen deficiency leading to phase separation. Therefore, we have restricted our detailed physical studies to the stoichiometries $0.0 \leq x \leq 0.5$. We will discuss the reasons for differences between our data and that reported by Johnston and Sestrich[39] and Eylem et al.[38]

## Experimental Section

**Synthesis.** All materials, and the synthesis, of $LaTiO_3$, $ATiO_3$, and $La_{1-x}A_xTiO_3$ ($0.0 \leq x \leq 1.0$) have been described previously.[4]

**Structure.** X-ray powder diffraction data were obtained using an Enraf-Nonius Guinier camera equipped with a Johansson monochromator (Cu $K\alpha_1$ radiation). Finely ground samples were placed on a piece of cellophane tape with 5–10% silicon added as an internal standard. By fitting to a quadratic function, the five observed silicon diffraction lines were correlated to their known diffraction angles. A least-squares fitting program was used to calculate lattice parameters for the series (Table I). The lattice parameters of $BaTiO_3$ and $LaTiO_3$ are in agreement with their respective literature values. Tables of indexed powder diffraction patterns for $La_{1-x}Ba_xTiO_3$ ($0.0 < x \leq 0.5$) are available as supplementary material (see paragraph at end of paper).

A second set of X-ray diffraction data was obtained on a Siemens D-500 powder diffractometer with Cu $K\alpha$ radiation. The powder data, shown in Figure 1, were examined to check peak splitting, peak shapes, and intensity values. Powder X-ray diffraction data were obtained at room temperature for all samples.

**Oxygen Stoichiometry.** Oxygen stoichiometry was determined using a du Pont 2100 thermal analyzer. The samples were heated at 5 °C/min to 1000 °C under flowing $O_2$ (50 cc/min) and allowed to isotrack at 900 °C for 2 h to allow complete oxidation. The oxidation products were assumed to be $La_2Ti_2O_7$ and $BaTiO_3$ for the purpose of calculating the oxygen stoichiometry.

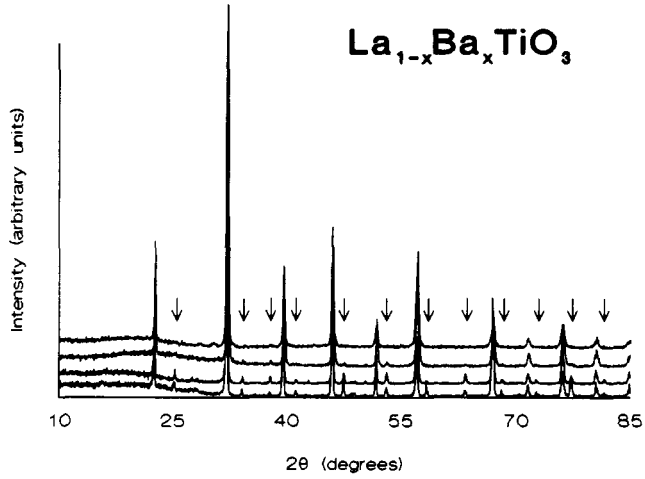


**Figure 1.** X-ray powder diffraction data for (from bottom to top) (a) $La_{0.95}Ba_{0.05}TiO_3$, (b) $La_{0.9}Ba_{0.1}TiO_3$, (c) $La_{0.8}Ba_{0.2}TiO_3$, and (d) $La_{0.7}Ba_{0.3}TiO_3$. The arrows indicate reflections due to the *Pbnm* structure type.

**Elemental Analysis.** Cation stoichiometries (La, Ba, Ti) were determined using a Cameca SX50 electron microprobe on alumina polished samples. $LaTiO_3$ was used as the standard for La and Ti analysis. $BaTiO_3$ was used as the standard for Ba analysis. Grain sizes were determined by backscattered electron images.

**Magnetic Susceptibility.** Temperature-dependent magnetic susceptibility was measured using a Quantum Design SQUID magnetometer. Samples were powdered and placed in evacuated quartz tubes for measurement. The samples with composition $0.0 \leq x \leq 0.05$ were cooled in an applied field of 1 T to 5 K. The magnetization vs temperature data were taken in an applied field of 10 G (5–170 K) and 1 T (170–300 K). For $x = 0.1, 0.2$, the applied field was 1000 G from 5–300 K. At compositions of $x > 0.2$, 1 T was applied from 5 to 300 K. All samples were screened for the Meissner effect at 5 K.

**Electrical Resistivity.** Temperature dependent dc resistivity was measured using a standard four-probe technique. Sample preparation was previously described.[4] Samples were measured from 15–300 K in 5 K increments. Reversal of current bias was used to minimize thermal voltages.

## Results and Discussion

**Synthesis.** The compounds in this study are prepared by arc melting a two-component mixture: $LaTiO_3$ and $BaTiO_3$. The two previous studies also use arc melting to make their materials, but the reactant mixtures in both studies contain more components. In the earlier study by Johnston et al. the $La_{1-x}Ba_xTiO_3$ compounds were prepared by arc melting $BaTiO_3$ with $La_2O_3 + Ti_2O_3$.[39] The authors report that the $Ti^{3+}$ analysis shows the materials to be somewhat oxidized. Oxidized samples could be the result of the formation of a solid solution of $La_{2/3}TiO_3$ and $BaTiO_3$ (high-temperature polymorph) in which both end members are cubic leading to a cubic solid solution. The synthesis of $La_{1-x}Ba_xTiO_3$ in a recent study by Eylem et al. is completed by the arc melting of $BaTiO_3$, $La_2O_3$, Ti metal, and $TiO_2$.[38] Our attempts to make $La_{1-x}Ba_xTiO_3$ using this method yielded small amounts of side products including $La_{2/3}TiO_3$. Better control over the product is achieved by reacting $LaTiO_3$ with $BaTiO_3$, as done in our study. This allows for more efficient mixing of the two components of similar structure type (perovskite) and allows for more homogeneous samples. In contrast to the work by Eylem et al. the samples with the composition $0.1 \leq x \leq 0.3$ appear to be single phase when prepared by arc melting the two-component mixture. Although we have

(33) Bazuev, G. V.; Shveikin, G. P. *Zh. Neorg. Khim.* **1977**, *22*, 1239.
(34) Ganguly, P.; Parkash, O.; Rao, C. N. R. *Phys. Status Solidi A* **1976**, *36*, 669.
(35) Bazuev, G. V.; Shveikin, G. P. *Fiz. Tverd. Tela.* **1975**, *11*, 3453.
(36) Kestigian, M.; Ward, R. *J. Am. Chem. Soc.* **1955**, *77*, 6199.
(37) Kestigian, M.; Ward, R. *J. Am. Chem. Soc.* **1954**, *76*, 6027.
(38) (a) Eylem, C.; Saghi-Szabo, G.; Chen, B.-H.; Eichorn, B.; Peng, J.-L.; Greene, R.; Salamanca-Riba, L.; Nahm, S. *Chem. Mater.* **1992**, *4*, 1038. (b) Robey, S. W.; Hudson, L. T.; Eylem, C.; Eichorn, B. *Phys. Rev. B: Condens. Matter* **1993**, *48*, 562.
(39) Johnston, W. D.; Sestrich, D. *J. Inorg. Nucl. Chem.* **1961**, *20*, 32.

**Table II. Cation and Oxygen Stoichiometries for $La_{1-x}Ba_xTiO_3$ Obtained from Electron Microprobe and Thermal Gravimetric Analysis, Respectively**

| theoretical | experimental | theoretical | experimental |
|---|---|---|---|
| $LaTiO_3$ | $La_{1.07(6)}TiO_{2.98}$ | $La_{0.70}Ba_{0.30}TiO_3$ | $La_{0.72(2)}Ba_{0.29(3)}TiO_{2.99}$ |
| $La_{0.95}Ba_{0.05}TiO_3$ | $La_{0.98(2)}Ba_{0.05(1)}TiO_{2.99}$ | $La_{0.60}Ba_{0.40}TiO_3$ | $La_{0.65(3)}Ba_{0.38(4)}TiO_{2.99}$ |
| $La_{0.90}Ba_{0.10}TiO_3$ | $La_{0.91(2)}Ba_{0.10(1)}TiO_{2.99}$ | $La_{0.50}Ba_{0.50}TiO_3$ | $La_{0.51(8)}Ba_{0.51(7)}TiO_{3.01}$ |
| $La_{0.80}Ba_{0.20}TiO_3$ | $La_{0.82(3)}Ba_{0.20(2)}TiO_{3.00}$ | | |

not performed HREM on the samples, the structure change from *Pbnm* to *Ibmm* is allowed by Landau theory, and we do not expect a biphasic mixture. It is probable that samples prepared with four components, $BaTiO_3$, $La_2O_3$, Ti metal, and $TiO_2$, are biphasic as a result of a mixture of the $La_{1-x}Ba_xTiO_3$ (orthorhombic) and $La_{2/3-x}Ba_xTiO_3$ (cubic) structure types. We have previously assigned the structures of $La_{1-x}Ba_xTiO_3$ to be in the orthorhombic *Pbnm* space group for $x \leq 0.20$ and the orthorhombic *Ibmm* space group for $0.2 < x \leq 0.5$. The structures for this study and the two previous studies[38,39] have been assigned based on powder X-ray diffraction data. Powder neutron data unequivocally confirmed the *Ibmm* structure type in the $La_{1-x}Sr_xTiO_3$ system.[4] On the basis of the result of the $La_{1-x}Sr_xTiO_3$ system, the splitting of several peaks in the powder X-ray diffraction pattern, and abrupt changes in the cell volume, we have indexed the compounds on an orthorhombic lattice.

**Structure.** The lattice parameters for the series are shown in Table I. Indexed powder patterns are given as supplemental materials. $LaTiO_3$ crystallizes in the $GdFeO_3$ (*Pbnm*) structure type.[26,31] The $La_{1-x}Ba_xTiO_3$ solid solution maintains the $GdFeO_3$ structure type until $x = 0.20$. This is in good agreement with the Goldschmidt tolerance factor proposed for this structure type.[40]

In addition, the *Pbnm* space group consists of two substructures: O′-orthorhombic and O-orthorhombic. The O′-orthorhombic is equal to the O-orthorhombic structure with a superimposed Jahn–Teller distortion. The O′-orthorhombic substructure is characterized by a $c_0/a_0$ ratio that is less than $\sqrt{2}$. The Jahn–Teller distortion for $LaTiO_3$ consists of a compression along the *c* axis. In the $La_{1-x}Ba_xTiO_3$ series, the Jahn–Teller distortion is no longer present by $x = 0.05$. Figure 1 clearly shows the weak peaks characteristic of the *Pbnm* structure for the $x = 0.05, 0.10, 0.20$ compositions. The samples $0.30 \leq x \leq 0.50$ are indexed in the *Ibmm* space group. As with the $La_{1-x}Sr_xTiO_3$ series, the *a* and *b* parameters converge until they are the same within error and then diverge. This coincides with a rearrangement of the $TiO_6$ octahedra. The difference between the *Pbnm* and *Ibmm* space groups is due to the different tilting modes of the $TiO_6$ octahedra. The *Pbnm* structure type is characterized by corner-shared $TiO_6$ octahedra which are tilted along the [001] axis and within the (001) plane. The octahedra in the *Ibmm* structure are tilted only along the [001] direction. This difference in tilting accounts for two slightly inequivalent Ti–O–Ti angles in the *Pbnm* structure but two widely different Ti–O–Ti angles in the *Ibmm* structure. Although the Guinier powder pattern can be indexed as cubic, the orthorhombic *Ibmm* space group adequately accounts for the broadness of the peaks. In addition, splitting of the peaks is observed in the Guinier film data.

**Elemental Analysis.** Experimental stoichiometries for $La_{1-x}Ba_xTiO_3$ ($0.0 \leq x \leq 0.5$) are given in Table II. Electron microprobe was completed on 6–8 random points on each sample and the reported value is an average of the random points. The experimentally determined stoichiometries are the same as the theoretical stoichiometries within the quoted error. The errors given in Table II are the standard deviations of the 6–8 random points. The standard deviations give some indication of the homogeneity of the sample. The samples appear to be homogeneous with the exception of the $La_{0.5}Ba_{0.5}TiO_3$ sample. In the $Ce_{1-x}Ba_xTiO_3$ system, we noted heterogeneity's in samples with high $BaTiO_3$ concentration.[3] For samples with high $BaTiO_3$ concentration, we have attributed the inefficient mixing to the large size difference between the barium and rare-earth metal cations.

The samples studied will be referred to by their theoretical stoichiometries in this paper.

**Microstructure.** Figure 2 shows backscattered electron images of all the samples in this study except for $La_{0.8}Ba_{0.2}TiO_3$. The average grain size is approximately 20 μm for the $La_{0.95}Ba_{0.05}TiO_3$ (see Figure 2a) and increases with $BaTiO_3$ content until there are no detectable grain boundaries for $La_{0.6}Ba_{0.4}TiO_3$ (see Figure 2d). The white phase in the grain boundaries was qualitatively determined by EDAX (energy-dispersive analysis by X-rays) to be $La_2O_3$. The white phase only appears in the La-rich samples (see Figure 2a–c). Due to the uncontrolled fast cooling rate, the grain structure varies within individual samples. Figure 3 shows the grain structure from the interior (Figure 3a) and exterior (Figure 3b) sections of the $La_{0.8}Ba_{0.2}TiO_3$ melt.

**Magnetic Properties.** The susceptibility vs temperature (5–300 K) data for the $La_{1-x}Ba_xTiO_3$ ($0.1 \leq x \leq 0.5$) samples are shown in Figure 4. The samples are temperature independent down to 50 K and have a very small paramagnetic tail. $LaTiO_3$ is a canted antiferromagnet which shows a net ferromagnetic ordering at 150 K.[6,30] We have previously shown that the magnetic ordering is destroyed with the addition of a small amount (<5%) of $BaTiO_3$.[5] Figure 5 shows the magnetization vs field curves for $LaTiO_3$ and $La_{0.95}Ba_{0.05}TiO_3$. The magnetization vs field curve of $La_{0.95}Ba_{0.05}TiO_3$ shows a slight field dependence which indicates a small ferromagnetic component to the magnetism. The loss of magnetic ordering in $La_{0.95}Ba_{0.05}TiO_3$ is coincident with the loss of Jahn–Teller distortion. This is similar to the behavior noted in the $La_{1-x}Sr_xTiO_3$ series.[4]

Figure 6 shows the high-temperature (180–300 K) susceptibility vs temperature data for all the compositions studied. The high-temperature data show that the compositions are temperature independent which is indicative of their metallic character. The susceptibility does not decrease smoothly with increasing $BaTiO_3$ content (from top to bottom). Figure 7 shows $\chi_{m(300\ K)}$ plotted as of function of composition ($x$) for $La_{1-x}Ba_xTiO_3$ ($0.0 \leq x \leq 0.5$). The largest change is seen between the $x = 0.0$ and $x = 0.05$ sample as shown in Figure 7. The Pauli component of the temperature-independent susceptibility is proportional to the density of states (DOS) at the Fermi level. We have previously proposed for the $La_{1-x}Sr_xTiO_3$

(40) Goodenough, J. B. *Prog. Solid State Chem.* 1975, *B25*, 925.

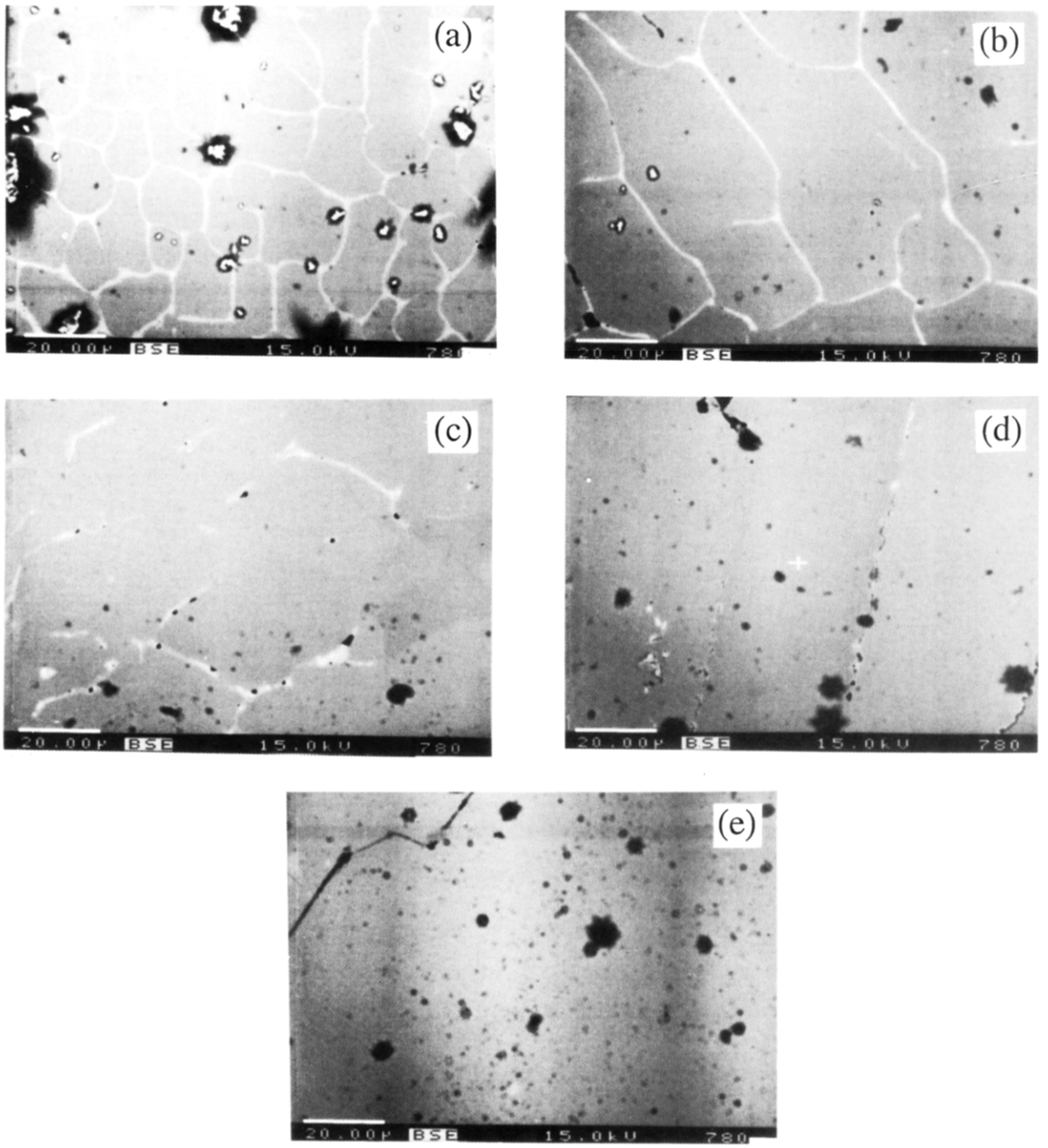


**Figure 2.** Electron microprobe micrographs of (a) $La_{0.95}Ba_{0.05}TiO_3$, (b) $La_{0.9}Ba_{0.1}TiO_3$, (c) $La_{0.7}Ba_{0.3}TiO_3$, (d) $La_{0.6}Ba_{0.4}TiO_3$, and (e) $La_{0.5}Ba_{0.5}TiO_3$. The scale given in the lower left corner of each micrograph is 20 $\mu$m.

series that the nonlinear drop in temperature-independent susceptibility, and therefore, the DOS is caused by changes in the band structure which coincide with crystal structure changes.[4] This is consistent with the electronic structure determined by photoemission and X-ray absorption spectroscopy.[41,42] This interpretation can also be successfully applied to the $La_{1-x}Ba_xTiO_3$ system. At $x = 0.05$, there is a structural change from the O′-orthorhombic to O-orthorhombic *Pbnm* structure types which is a result of the loss of Jahn–Teller distortion and an abrupt decrease in $\chi_{(300\ K)}$ is observed. There is a smooth decrease for $x = 0.05$–$0.5$ which is consistent with the removal of an electron from the $d_{xy}$ band.

**Electrical Properties.** Figures 8 and 9 show normalized resistivity vs temperature data for $La_{1-x}Ba_xTiO_3$. In random samples of the compositions studied, the data (see Figure 8) shows a resistive anomaly similar to that noted before in $Ba_{1-x}La_xTiO_3$ PTCR thermistors.[7–23,43] The occurrence of the resistive anomaly in this study did not appear to be dependent on composition as the effect was noted in various compositions. For example, Figure 8 shows the samples exhibiting the PTCR effect, while those exhibiting normal metallic behavior are shown in Figure 9. At a fixed composition, the PTCR effect only occurs

(41) Fujimori, A.; Hase, I.; Nakamura, M.; Namatame, H.; Fujishima, Y.; Tokura, Y.; Abbate, M.; de Groot, F. M. F.; Czyzyk, M. T.; Fuggle, J. C.; Strebel, O.; Lopez, F.; Domke, M.; Kaindl, G. *Phys. Rev. B: Condens. Matter* **1992**, *46*, 9841.

(42) Abbate, M.; de Groot, F. M. F.; Fuggle, J. C.; Fujimori, A.; Tokura, Y.; Fujishima, Y.; Strebel, O.; Domke, M.; Kaindl, G.; van Elp, J.; Thole, B. T.; Sawatzky, G. A.; Sacchi, M.; Tsuda, N. *Phys. Rev. B: Condens. Matter* **1991**, *44*, 5419.

(43) Peria, W. T.; Bratschum, W. R.; Fenity, R. P. *J. Am. Ceram. Soc.* **1961**, *44*, 249.

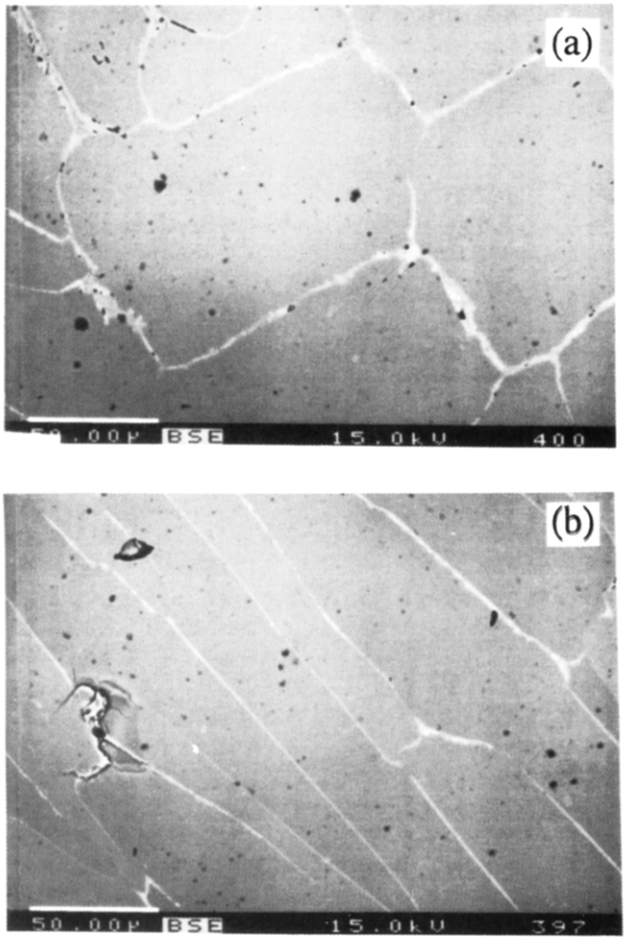


**Figure 3.** Electron microprobe micrographs of (a) $La_{0.8}Ba_{0.2}TiO_3$ (interior of melt) and (b) $La_{0.8}Ba_{0.2}TiO_3$ (exterior of melt). The scale given in the lower left corner of each micrograph is 50 $\mu$m.

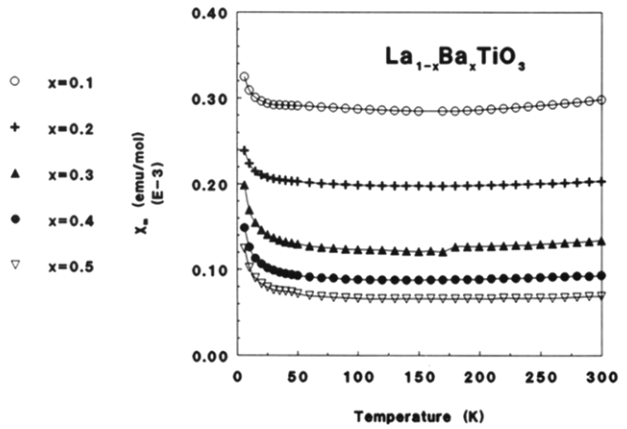


**Figure 4.** Temperature-dependent magnetic susceptibility (5–300 K) for (from top to bottom) (a) $La_{0.9}Ba_{0.1}TiO_3$, (b) $La_{0.8}Ba_{0.2}TiO_3$, (c) $La_{0.7}Ba_{0.3}TiO_3$, (d) $La_{0.6}Ba_{0.4}TiO_3$, and (e) $La_{0.5}Ba_{0.5}TiO_3$.

in random samples indicating that the anomaly is dependent on the sample preparation. Figures 8 and 9 show the data for the compositions studied with microprobe and whose electron micrographs are shown in Figures 2 and 3. As can be seen with these particular samples, the largest effect was observed in the $x = 0.3$ sample. The dependence of the PTCR effect on sample preparation conditions in $Ba_{1-x}La_xTiO_3$ has been noted previously.[7-11,14-23] However, the anomaly is shifted 120 °C lower than previously seen.[7-23,43] The grain sizes in the

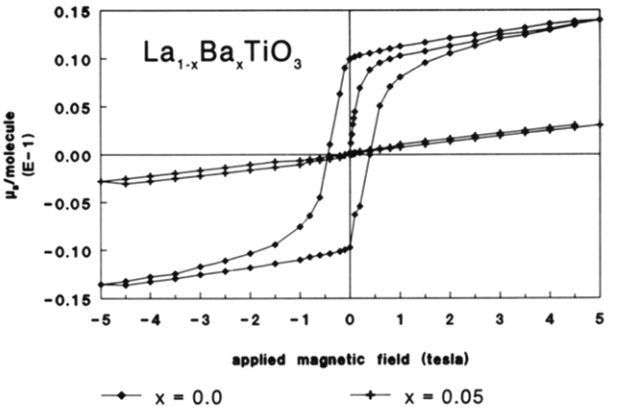


**Figure 5.** Field-dependent magnetic susceptibility (−5 to 5 T) for (a) $LaTiO_3$ and (b) $La_{0.95}Ba_{0.05}TiO_3$.

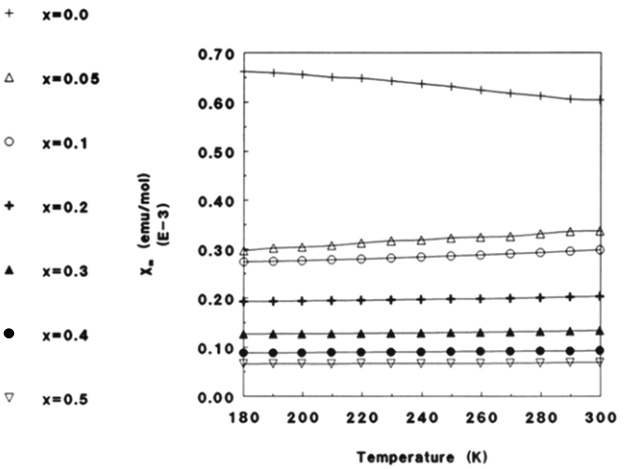


**Figure 6.** Temperature-dependent magnetic susceptibility (180–300 K) for (from top to bottom) (a) $LaTiO_3$, (b) $La_{0.95}Ba_{0.05}TiO_3$, (c) $La_{0.9}Ba_{0.1}TiO_3$, (d) $La_{0.8}Ba_{0.2}TiO_3$, (e) $La_{0.7}Ba_{0.3}TiO_3$, (f) $La_{0.6}Ba_{0.4}TiO_3$, and (g) $La_{0.5}Ba_{0.5}TiO_3$.

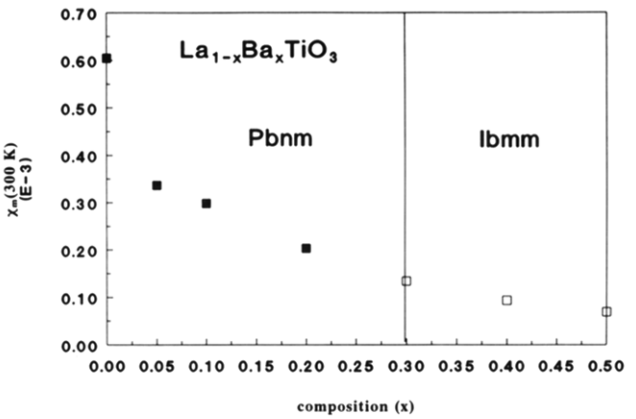


**Figure 7.** Room-temperature susceptibilities vs composition for $La_{1-x}Ba_xTiO_3$.

samples studied were ≥20 $\mu$m while the average ideal grain size for PTCR materials is ≤10 $\mu$m.[14-23] It is also interesting to note that the PTCR characteristics are exhibited in certain $La_{0.95}Ba_{0.05}TiO_3$ samples (see Figure 8a) whereas it has previously been noted only in samples with high Ba concentration.[7-23,43]

One theory suggests that the PTCR effect is a result of the strain incurred in the tetragonal–cubic transition which in turn changes the contact resistance between the crystallites.[43] $BaTiO_3$ assumes a tetragonal structure (*P4mm*) at room temperature and a cubic structure above 120 °C. The PTCR effect in doped $BaTiO_3$ samples is

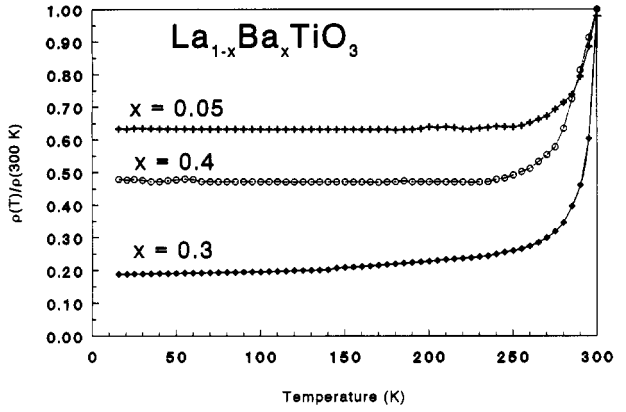


**Figure 8.** Normalized resistivity vs temperature for (a) $La_{0.95}Ba_{0.05}TiO_3$, (b) $La_{0.7}Ba_{0.3}TiO_3$, and (c) $La_{0.6}Ba_{0.4}TiO_3$.

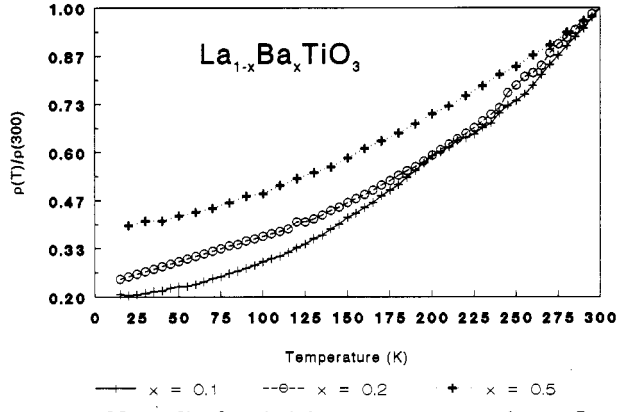


**Figure 9.** Normalized resistivity vs temperature for (a) $La_{0.9}Ba_{0.1}TiO_3$, (b) $La_{0.8}Ba_{0.2}TiO_3$, and (c) $La_{0.5}Ba_{0.5}TiO_3$.

usually observed around the tetragonal-to-cubic transition temperature. It is known that doped $BaTiO_3$ samples, which show the PTCR effect, exhibit diffuse phase transition characteristics which are attributed to microheterogeneity in composition.[14] The PTCR behavior observed in the $La_{1-x}Ba_xTiO_3$ samples in this study may be a result of the preparation technique (are melting) used. Due to the extremely fast cooling rate of the reaction, it is possible that the sample, or a portion of the sample, assumes a metastable cubic structure at room temperature. The strain in the arc-melted cubic sample should rapidly increase upon cooling during the experiment and give rise to the PTCR effect.

The PTCR effect has also been attributed to nonstoichiometry in studied samples.[14,15,17,18] The presence of $La_2O_3$ in the grain boundaries of the La-rich samples indicates some nonstoichiometry in the sample. However, the occurrence of the effect in the samples measured is not related to this nonstoichiometry since the PTCR behavior is also noted in samples where the $La_2O_3$ phase is not present ($La_{0.6}Ba_{0.4}TiO_3$). It is likely that the PTCR behavior in these samples is due to strain, but the technique of arc melting precludes controlled preparation conditions.

The samples which do not show the PTCR effect are metallic as in the $La_{1-x}Sr_xTiO_3$ compounds and the normalized temperature dependent resistivities are shown in Figure 9.[4] All the samples have room temperature resistivities in the $10^{-2}$–1 Ω cm range.

**Acknowledgment.** We thank Professor Robert N. Shelton for use of the SQUID magnetometer, thermal analyzer, and X-ray diffractometer. We thank Drs. Peter Schiffman and Sara Roeske for assistance with the microprobe measurements. We also thank Dr. B. Eichorn for useful discussion and a preprint of ref 38b. This work was supported by National Science Foundation Solid State Chemistry Grant DMR-8913831, -9201041.

**Supplementary Material Available:** Tables of indexed powder diffraction patterns for $La_{1-x}Ba_xTiO_3$ ($0.0 < x \leq 0.5$) (8 pages). Ordering information is given on any current masthead page.